Brain Pathology ISSN 1015–6305

RESEARCH ARTICLE

Abnormal development of the inferior temporal region in fetuses with Down syndrome

Sandra Guidi[1]; Andrea Giacomini[1]; Fiorenza Stagni[1]; Marco Emili[1]; Beatrice Uguagliati[1]; Maria Paola Bonasoni[2]; Renata Bartesaghi[1]

[1] Department of Biomedical and Neuromotor Sciences, University of Bologna, Bologna, Italy.
[2] Pathology Unit, Azienda Unità Sanitaria Locale – IRCCS, Reggio Emilia, Italy.

Keywords
calretinin, cellularity, Down syndrome, fetal brain, neurogenesis, temporal lobe.

Corresponding author:
Renata Bartesaghi, Department of Biomedical and Neuromotor Sciences, Physiology Building, Piazza di Porta San Donato 2, I-40126 BOLOGNA BO, Italy (E-mail: *renata.bartesaghi@unibo.it*)

Received 17 October 2017
Accepted 4 March 2018
Published Online Article Accepted 6 March 2018

doi:10.1111/bpa.12605

Abstract

Down syndrome (DS) is a genetic condition associated with impairment in several cognitive domains. Previous evidence showed a notable neurogenesis reduction in the hippocampal region of DS fetuses, which may account for the impairment of declarative memory that characterizes DS starting from early life stages. The fusiform gyrus (FG) and the inferior temporal gyrus (ITG) play a key role in visual recognition memory, a function that is impaired in children and adults with DS. The goal of the current study was to establish whether fetuses with DS (17–21 weeks of gestation) exhibit neuroanatomical alterations in the FG and ITG that may underlie recognition memory impairment. We found that the FG and ITG of fetuses with DS had a reduced thickness and fewer cells in comparison with euploid fetuses. Moreover, DS fetuses had fewer cells expressing the neuronal marker NeuN than euploid fetuses, but a similar number of cells expressing the astrocytic marker GFAP and, consequently, a higher percentage of astrocytes. Immunohistochemistry for calretinin (CR), a marker of GABAergic interneurons, showed that in DS fetuses the ratio of CR-positive vs. CR-negative cells was greater than in euploid fetuses, both in the FG (+77%) and ITG (+61%). An increased ratio of CR-positive vs. CR-negative cells was also found in the entorhinal cortex, hippocampus and dentate gyrus. Results provide novel evidence that the FG and ITG of DS fetuses exhibit numerous developmental defects. These defects may underlie the functional alterations in visual recognition memory observed in children with DS.

INTRODUCTION

Down syndrome (DS), a genetic condition due to triplication of chromosome 21, is associated with impairment in several cognitive domains starting from the earliest phases of development. IQ in people with DS usually falls in the moderately severe intellectual disability range (IQ = 25–55) and mental age is rarely over 8 years (10, 32, 33). The IQ in DS is not constant lifetime long but it progressively decreases with age and an early deceleration occurs between the age of 6 months and 2 years, with a further decline in adolescents. Children with DS exhibit incomplete and delayed acquisition of motor, linguistic, cognitive and adaptive functions, compared with developing peers of the same mental age and a risk of a higher level of psychopathology.

Children with DS have normal learning abilities for tasks requiring implicit memory but exhibit selective impairment of explicit memory, with poor information encoding, impaired retrieval abilities and attention deficits (8, 34). When tested for learning tasks that specifically assess the state of function of the hippocampal systems, infants and adults with DS show a severe impairment (25). A considerable body of data from both animal and human studies has implicated the medial temporal lobe in memory processes. Among the structures in this region, most research has focused on the role of the hippocampal region that is formed by the hippocampus, dentate gyrus, subiculum, presubiculum and entorhinal cortex. It is well established that the hippocampal formation (hippocampus plus dentate gyrus) is fundamental for long-term explicit memory for places and events. Previous evidence from our group showed a notable reduction in the number of proliferating cells and overall cellularity in the hippocampal formation and other structures of the hippocampal region of DS fetuses (20). Moreover, fetuses with DS exhibited a reduced number of neurons and a relative increase in the number of astrocytes, suggesting that these early neurodevelopmental alterations may account for the alterations of explicit memory in children with DS.

Visual recognition memory is the ability to judge the prior occurrence of stimuli and is fundamental to our ability to record events and to guide prospective behavior. The human ventral temporal cortex is a key-structure in high-level visual processing, such as face perception and object recognition. In particular, the fusiform gyrus and the inferior temporal gyrus play a key role in visual recognition memory, that is, they are involved in recognizing and interpreting information about objects and faces [see (6, 36)]. They receive visual

Table 1. Cases of the present study.

Case				Age (weeks)	Sex	CRL (cm)	BW (g)
Euploid fetuses							
C118*	^	§	+	17	M	13	180
C164*	^	§		19	F	14	285
C27*	^	§		20	F	17	230
C101	^		+	20	M	15	340
C104*	^		+	20	M	15	330
C178*	^	§		21	M	n.a.	n.a.
Down syndrome fetuses							
C203*	^	§	+	18	F	14.5	210
C166*	^	§		19	F	14	240
C133*	^	§		20	M	16	300
C156	^		+	20	M	17	385
C46*	^	§		21	M	22	355
C77*	^		+	21	F	17.5	300

List of the cases used in the present study. Cases labeled with an asterisk are the same as in a previous study (20). Cases labeled with ^ were used for stereology; cases labeled with § were used for NeuN, GFAP, S100B and vimentin immunohistochemistry; cases labeled with + were used for CR immunohistochemistry. Age refers to gestational age in weeks. CRL, crown-rump length; BW, body weight; F, female; M, male; n.a., not available.

input from the occipital lobe and, thus, they are a part of the ventral visual pathway, which identifies "what" things are. They are thought to be responsible for combining visual features to form representations of complex shapes (6, 24). Visual recognition memory is impaired in children and adults with DS (15, 35), suggesting that this defect may be due to alterations of the fusiform gyrus and inferior temporal gyrus. Based on these premises, the goal of the current study was to establish whether fetuses with DS exhibit early neurodevelopmental alterations in the fusiform gyrus and inferior temporal gyrus that may account for recognition memory impairment.

METHODS

Subjects

For this study, we used fetuses between 17 and 21 gestational weeks (GW). Brains were obtained after prior informed consent from the parents and according to procedures approved by the Ethical Committee of the St. Orsola-Malpighi Hospital, Bologna, Italy and by the Ethical Committee of the Azienda Unità Sanitaria Locale, Reggio Emilia, Italy. Regulations of the Italian Ministry of Health and the policy of Declaration of Helsinki were followed. All fetuses derived from legal abortion and were collected with an average post-mortem delay of approximately 2 h. Six euploid fetuses with no obvious developmental or neuropathological abnormalities and six DS fetuses were used (Table 1). Some of the fetuses (cases marked with an asterisk in Table 1) are the same used in a previous study (20). Trisomy was karyotypically proven from the results of genetic amniocentesis procedures. All cases were classical trisomy 21 (free trisomy). Autopsies were performed at the Institute of Pathology of the St. Orsola Malpighi Hospital (Bologna, Italy) or at the Azienda Unità Sanitaria Locale (Reggio Emilia, Italy). The gestational age of each fetus was estimated by menstrual history and crown-rump length.

Histological procedures

Whole brains were fixed by subdural perfusion with Metacarnoy fixative (methyl alcohol:chloroform:acetic acid 6:1:1) injected through the anterior and posterior fontanelles. After 24–48 h the brains were removed, the region of the right hemisphere caudal to the mammillary bodies was dissected out and coronally sectioned in order to obtain three to four blocks with a thickness of 2–3 mm. These blocks encompassed the brain region that stretches from the beginning to the end of the hippocampal region. The blocks were post-fixed in 4% buffered formaldehyde for 5–7 days and embedded in paraffin according to standard procedures. The first block was cut so as to obtain, in addition to 8- or 12-μm thick sections, five to six series of three-four 4- to 5-μm thick sections, 200 μm apart. The 8- to 12-μm thick sections were Nissl-stained and previously used for morphometric reconstruction of the hippocampal region (20).

NeuN, GFAP, S100B, vimentin and calretinin immunohistochemistry

Two to four sections were immunostained using monoclonal anti-NeuN (neuron specific nuclear protein) from Chemicon International, The United States (dilution 1:200; clone A60). Three to five sections were stained for glial fibrillary acidic protein (GFAP) using a monoclonal antibody from Sigma Chemical Co., The United States (dilution 1:1600; clone G-A-5). Two to three sections were immunostained using polyclonal anti-S100 antibody-Astrocyte marker from Abcam, Cambridge, The United Kingdom (dilution 1:100). Two to three sections were immunostained using monoclonal anti-Vimentin antibody from Sigma Aldrich (dilution 1:100; clone V9). Four to six sections were immunostained for calretinin (CR) using mouse anti-Calretinin RTU, from Novocastra (dilution 1:300; clone 5A5). Sections were retrieved with citrate buffer pH 6.0 at 98°C for 40 min before incubation with their proper antibody. Sections immunostained for NeuN, GFAP and Calretinin were counterstained with Mayer's Hematoxylin.

Nomenclature

In the adult brain, the fusiform gyrus is delimited medially by the collateral sulcus (whose anterior end is called rhinal sulcus) and laterally by the fusiform fissure. The inferior temporal gyrus is delimited medially by the fusiform fissure and laterally by a sulcus demarcating the border with the medial temporal gyrus. In the fetuses used here (GW17–GW21), a rhinal sulcus was recognizable at rostral level of the hippocampal region. Going caudally, the rhinal sulcus became less prominent and was replaced by a small but recognizable collateral sulcus or by a small "indentation," most likely representing the incipient collateral sulcus. Thus, the border between the parahippocampal gyrus and the adjacent regions of the ventral temporal lobe was recognizable (see for instance Figure 1A). At the fetal ages examined here, however, a fusiform fissure and a sulcus demarcating the border between the inferior and middle temporal gyrus were not detectable. Therefore we defined as fusiform gyrus (FG) the region that extends from the collateral sulcus to the point where the cortical plate undergoes a thickness increase (Figure 1A) and defined as inferior temporal gyrus (ITG) the region that stretches from the FG to the point where the cortex undergoes an upward rotation (Figure 1A). The term collateral

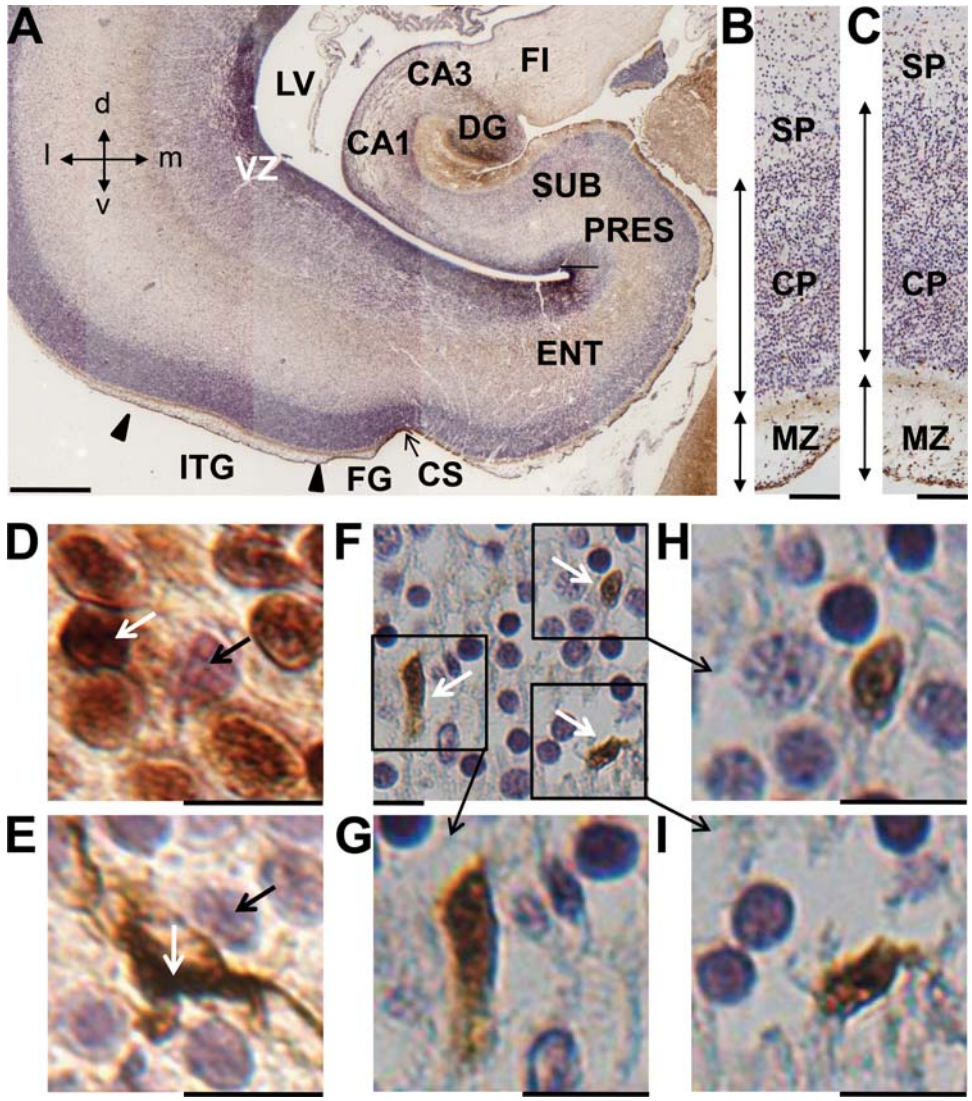

Figure 1. A–C. Low-magnification image (A) of a coronal section across the fetal temporal region and higher magnification images of the fusiform gyrus (B) and inferior temporal gyrus (C). The arrowheads in (A) mark the borders of the inferior temporal gyrus. Sections were immunostained for calretinin (brown color) and counterstained with hematoxylin (purple color). **D,E**. Examples of sections immunostained for NeuN (D) or GFAP (E) and counterstained with hematoxylin in the inferior temporal gyrus. The white arrow in (D) and (E) indicates a cell immunopositive for NeuN (D) and GFAP (E). The black arrow in (D) and (E) indicate a cell immunonegative for NeuN (D) and GFAP (E). **F**. Examples of cells immunostained for calretinin (white arrows) in the inferior temporal gyrus. Higher magnification images of the boxed areas in (F) are reported in (**G–I**). Images in (A–C) are from case C118 (GW 17) and images in (D–I) are from case A178 (GW 21). Calibrations: A = 1000 μm; B–C = 100 μm; D–I: 10 μm. Abbreviations: CA1, CA3, hippocampal fields; CP, cortical plate; CS, collateral sulcus; d, dorsal; DG, dentate gyrus; ENT, entorhinal cortex; FG, fusiform gyrus; FI, fimbria; ITG, inferior temporal gyrus; l, lateral; LV, lateral ventricle; m, medial; MZ, marginal zone; PHG, parahippocampal gyrus; PRES, presubiculum; SP, subplate; SUB, subiculum; v, ventral; VZ, ventricular zone.

sulcus of this study indicates the rhinal sulcus plus the collateral sulcus proper and the term hippocampal region corresponds to the hippocampal formation and parahippocampal gyrus.

Measurements

Image acquisition

A light microscope (Leitz) equipped with a motorized stage and focus control system and a color digital camera (Coolsnap-Pro; Media Cybernetics, Silver Spring, MD, USA) were used to take bright field images. Measurements were carried out using the Image Pro Plus software (Media Cybernetics, Silver Spring, MD, USA).

Density and percentage of NeuN- and GFAP-positive cells

In sections processed for NeuN immunohistochemistry and counterstained with Mayer's Hematoxylin, the nuclei of neurons were heavily stained in brown, while cells that did not express NeuN

exhibited a pale purple nuclear staining (Figure 1D). In sections processed for GFAP immunohistochemistry and counterstained with Mayer's Hematoxylin, the cytoplasm around the nucleus and the processes of astrocytes appeared stained in brown while the other cells exhibited only a pale purple nuclear staining (Figure 1E). In the series of sections processed for NeuN or GFAP immunohistochemistry, eight snaps (size: 260 × 195 μm) per section were randomly acquired across the total thickness and mediolateral extent of the cortical plate of the FG and ITG, respectively (objective: ×40, 0.70 NA; final magnification: ×500). In each acquired image, we counted all NeuN-positive and NeuN-negative cells and GFAP-positive and GFAP-negative cells. The total number of counted cells per snap ranged between 150 and 250. The number of NeuN- or GFAP-immunopositive cells was expressed in terms of (i) density per mm^2 and (ii) percentage of NeuN-positive or GFAP-positive cells over total number of cells per mm^2 (immunopositive plus immunonegative cells). The percentage of cells that expressed NeuN plus that of the cells that expressed GFAP was lower than 100%, indicating the presence of a population of cells with an undetermined phenotype. The percentage of cells with an undetermined phenotype was multiplied by the number of cells per mm^2 counted in the sections immunostained for NeuN, in order to obtain the density of cells with an undetermined phenotype.

Density and percentage of S100B- and vimentin-positive cells

Since the number of these cells in the cortical plate was very low, in sections processed for S100B or vimentin immunohistochemistry we acquired images of the whole region of interest by exploiting the tiling function of Image Pro Plus software (objective: ×25, 0.70 NA; final magnification ×312). In images of the FG and ITG, a series of areas enclosing the whole thickness of the cortical plate (width: 300–400 μm; height: 400–800 μm) were manually traced at different medio-lateral sites of the FG (2–3 areas per section) and ITG (3–4 areas per section). All immunopositive cells within these areas were counted (∼40–60 S100B-positive cells and ∼6–30 vimentin-positive cells per sampled area). The number of S100B- or vimentin-immunopositive cells was expressed in terms of (i) density per mm^2 and (ii) percentage over total number of cells/mm^2 counted in the sections immunostained for NeuN.

Density and percentage of CR-positive cells

Since the number of CR-positive cells was relatively low, in sections processed for CR immunohistochemistry we acquired images of the whole region of interest. We separately acquired images of the FG, ITG, entorhinal cortex (ENT), dentate gyrus (DG) and field CA1 at the focal plane at which the largest number of cells was recognizable. In order to count CR-positive and CR-negative cells in the FG, ITG and ENT, a series of approximately rectangular areas enclosing the whole thickness of the cortical plate (width: 60–100 μm; height: 400–800 μm) were manually traced at different mediolateral sites of the FG (3–6 areas per section), ITG (6–8 areas per section) and ENT (2–3 areas per section). All CR-positive and CR-negative cells within these areas were counted (total number of counted cells ∼400–600 per sampled area). We additionally counted the number of CR-positive and CR-negative cells in manually traced areas (size: ∼40 000–80 000 μm^2) in the marginal zone of the FG and ITG (number of counted cells ∼100–200 cells per area). In order to count CR-positive and CR-negative cells in the DG, an area enclosing the granule cell layer (GR) and an area enclosing the molecular layer (MOL) were manually traced. All CR-positive and CR-negative cells in the GR and all CR-positive cells in the MOL were counted. A total of approximately 500–1000 cells were counted in the GR and of 150–350 in the MOL per section. CR-positive and CR-negative cells were counted in the pyramidal layer and stratum radiatum of field CA1. To this purpose, a series of areas (3–6 areas per section) enclosing the whole thickness of stratum pyramidale (size: ∼4000–7000 μm^2) and of stratum radiatum (size: ∼30 000–50 000 μm^2) were manually traced along the whole extent of field CA1 (from the border with field CA3 to the border with the subiculum). All CR-positive and CR-negative cells within these areas were counted (total number of counted cells ∼40–80 per sampled area in stratum pyramidale and ∼40–80 per sampled area in stratum radiatum). The number of CR-positive and CR-negative cells was expressed in terms of (i) density per mm^2 and (ii) ratio of CR-positive vs. CR-negative cells.

Total cell density and thickness of the cortical plate in the FG and ITG

The number of immunopositive and immunonegative cells counted in the section processed for NeuN and CR immunohistochemistry (see above) was summed, divided by the size of the sampled area and expressed as number of cells/mm^2. In sections processed for NeuN or CR immunohistochemistry, the thickness of the cortical plate was measured at 3–4 random locations along the mediolateral extent of the FG and ITG in images taken at a final magnification of ×125.

Statistical analysis

Results are presented as mean ± standard deviation (SD). Statistical analysis was carried out using the two-tailed Student's *t*-test. A probability level of $P \leq 0.05$ was considered to be statistically significant.

RESULTS

Cytoarchitecture and cellularity in the FG and ITG of fetuses with DS

At the gestational ages examined here (GW 17–21) the fusiform gyrus (FG) and the inferior temporal gyrus (ITG) exhibited a single thick cell layer (cortical plate). The cortical plate appeared as a relatively homogeneous band of cells where individual layers were not recognizable. Observation of Figure 2A shows that in the cortical plate of a typical fetus cells exhibited an ordered organization, giving origin to sort of columns. This organization was more evident in the outer part of the cortical plate (Figure 2A). In contrast, in the cortical plate of a DS fetus of similar gestational age, cells were more sparsely arranged and a radial organization was missing (Figure 2A). The cortical plate forms according to an inside-outside design. Namely, the oldest cells settle to the deepest part of the cortical plate, while the younger cells migrate to more superficial parts of the cortical plate. The migration of cells from their site of origin, the ventricular zone (VZ) and subventricular zone (SVZ), is

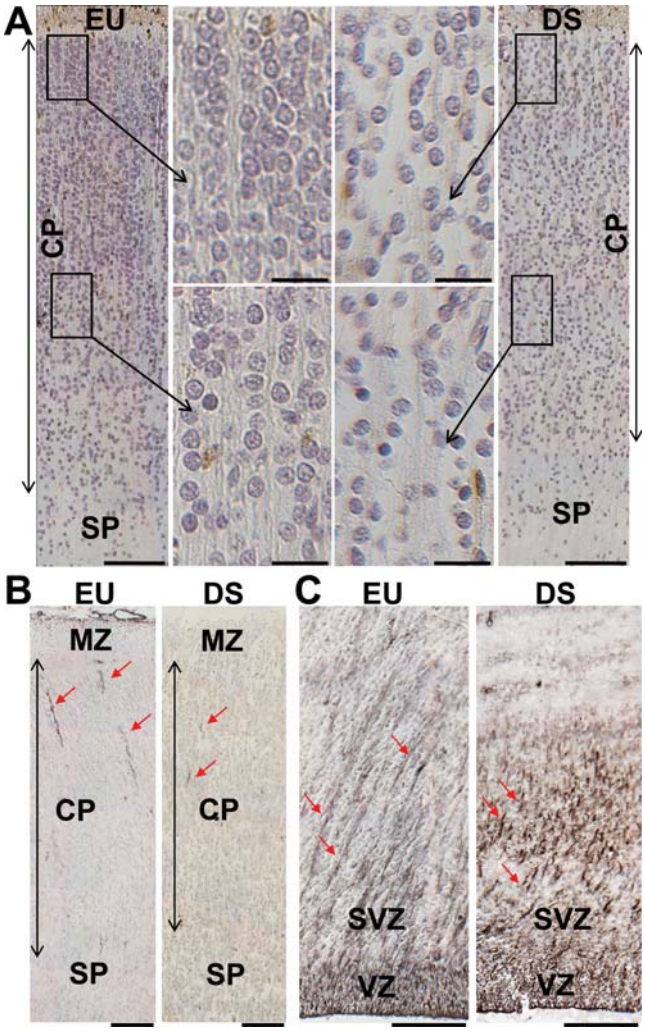

Figure 2. *Cytoarchitecture of the fusiform gyrus and inferior temporal gyrus in DS and euploid fetuses.* **A**. Sections immunostained for calretinin and counterstained with hematoxylin from the inferior temporal gyrus of a euploid fetus (image on the left) and a DS fetus (image on the right) at GW21. Images in the middle are higher magnification of the boxed areas. Note the radial organization of the cortical plate of the euploid fetus and the more disorganized appearance and hypocellularity of the cortical plate of the DS fetus. Calibrations = 100 μm (low magnification images); 20 μm (high magnification images). **B,C**. Sections immunostained for vimentin from the cortical plate (B) and ventricular region of the inferior temporal gyrus (C) at GW21. The red arrows indicate processes of radial glia cells. Note the ordered organization of radial glia processes in the ventricular zone/subventricular zone of the euploid fetus. Calibrations = 100 μm. Abbreviations: CP, cortical plate; EU, euploid; DS, Down syndrome; MZ, marginal zone: SP, subplate; SVZ, subventricular zone; VZ, ventricular zone.

guided by the processes of radial glia cells. These cells have their cell bodies in the VZ and extend their processes to the outermost part of the perspective cortical plate. The absence of a radial organization of cells in the cortical plate of the DS fetus (Figure 2A) suggests possible defects in the organization of radial glia processes. To clear this issue, sections from euploid and DS fetuses were immunostained with vimentin, a marker of radial glia. Only short segments of radial glia processes were detectable in the cortical plate (Figure 2B). This is consistent with previous evidence showing that while radial glia fibers span the whole thickness of the cerebral mantle and reach the pial surface in fetuses at GW 10–16, the proportion of radial glial cell processes covering the whole thickness of the cerebral mantle declines with age (GW 18–35) (12, 22). Numerous radial glia processes, however, were detectable in the VZ/SVZ. In euploid fetuses, these processes had an ordered elongated pattern and were oriented from the VZ/SVZ toward the cortical plate (Figure 2C). In contrast, in DS fetuses radial glia processes had a disorganized pattern and lacked a clear orientation toward the cortical plate (Figure 2C). This suggests that a similar disorganization is retained in the cortical plate, which may account for the sparse distribution of cell in the cortical plate of DS fetuses.

Figures 2A and 3A,B show that both in the FG and ITG cell density and cortical thickness were patently reduced in fetuses with DS in comparison with typical fetuses matched by age. Quantification of the thickness of the cortical plate showed that in fetuses with DS it was significantly thinner (Figure 3C,D) in comparison with euploid fetuses both in the FG (−22%) and ITG (−18%). An evaluation of the number of cell profiles per unit area showed that fetuses with DS had a significantly reduced cell density in the FG (−32%) and ITG (−22%) than euploid fetuses (Figure 3C,D). Taken together these data suggest that the FG and ITG of DS fetuses have a reduced cellularity due to a reduction both in the thickness of the cortical plate and number of cells per unit area.

Density and percentage of neurons and astrocytes in the FG and ITG of fetuses with DS

To establish the neuronal or astrocytic phenotype of the cells populating the cortical plate in the FG and ITG we carried out immunohistochemistry for NeuN, a marker of mature neurons or GFAP, a marker of astrocytes. An evaluation of the percentage of NeuN- and GFAP-positive cells over total number of counted cells showed that the percentage of cells that expressed NeuN plus that of the cells that expressed GFAP was lower than 100%, indicating the presence of a population of cells of an undetermined phenotype. Both euploid and DS fetuses had a notably larger number of cells exhibiting a neuronal phenotype over total cell number in comparison with cells exhibiting an astrocytic phenotype or cells with neither of these phenotypes (Figure 4A,C). In absolute terms, DS fetuses had a reduced number of cells with a neuronal phenotype in comparison with euploid fetuses both in the FG (Figure 4A) and ITG (Figure 4C) but a similar number of cells with an astrocytic phenotype and with an undetermined phenotype (Figure 4A,C). A comparison of the percentage of cells of each phenotype showed that DS fetuses had a reduced percentage of cells with a neuronal phenotype in the FG (Figure 4B) but a higher percentage of cells with an astrocytic phenotype both in the FG and ITG (Figure 4B,D). No differences were found between euploid and DS fetuses in the percentage of cells with an undetermined phenotype (Figure 4B,D).

Since astrocytes can express S100B and/or vimentin, in sections processed for these markers we counted the number of S100B- and vimentin-positive cells in the cortical plate of the FG and ITG. We found that the density of S100B-positive cells was approximately 10 times lower than that of GFAP-positive cells (compare Figure

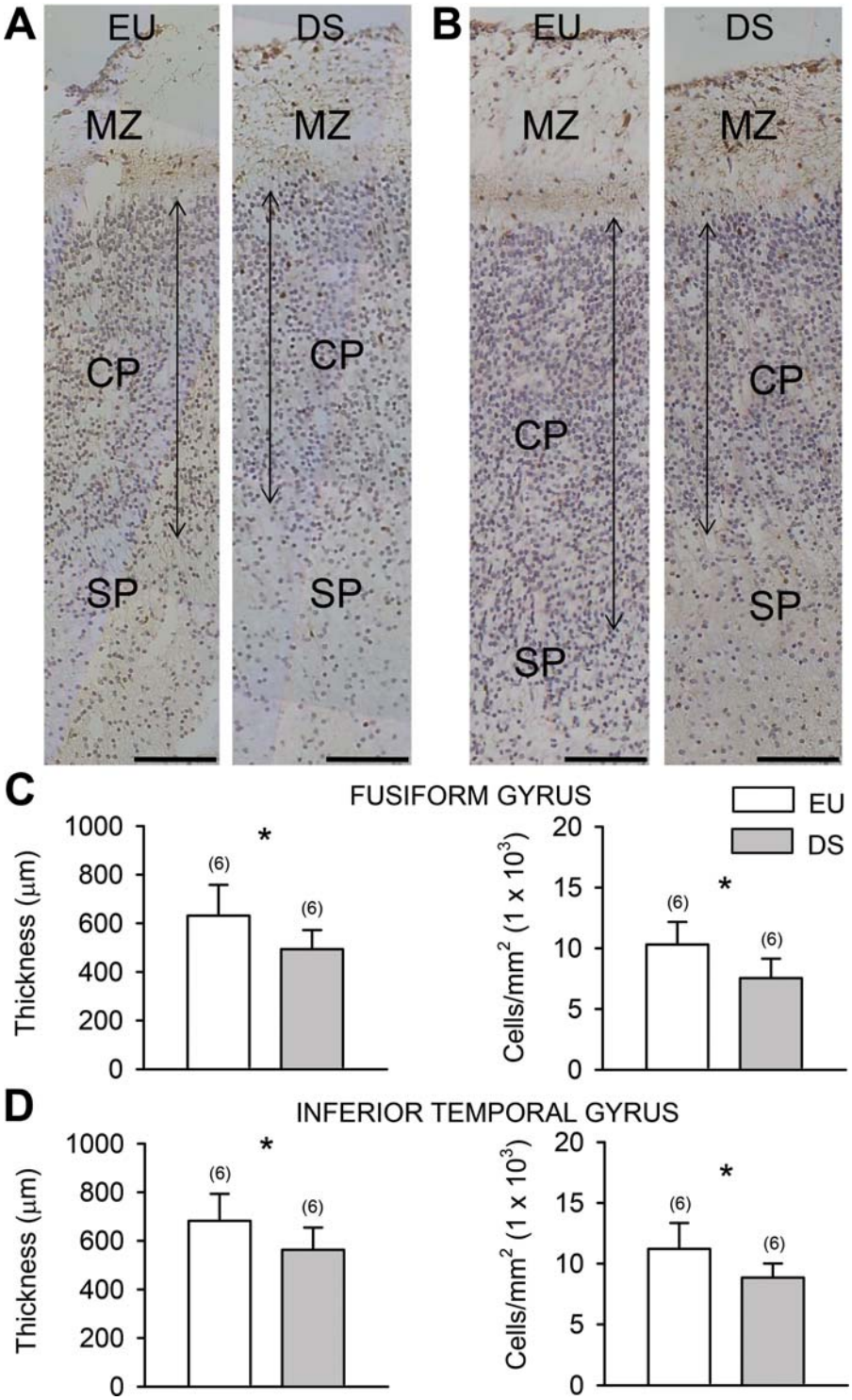

Figure 3. *Stereology of the fusiform gyrus and inferior temporal gyrus in DS and euploid fetuses*. **A,B**. Sections immunostained for calretinin and counterstained with hematoxylin from the fusiform gyrus (A) and inferior temporal gyrus (B) of a euploid (C118; GW17) and a DS fetus (C203; GW18). Note the reduced thickness of the cortical plate in the DS fetus. Calibration = 100 μm. **C,D**. Thickness of the cortical plate (panels on the left) and cell density, expressed as number of cells/mm^2 (panels on the right) of the fusiform gyrus (C) and inferior temporal gyrus (D) in DS (n = 6; GW 18–21) and euploid (n = 6; GW 17–21) fetuses. Values are mean ± SD. The number in parentheses indicates the number of samples analyzed for each experimental group. * $P < 0.05$ (two tailed *t*-test). Abbreviations: CP, cortical plate; EU, euploid; DS, Down syndrome; GW, gestational week; MZ, marginal zone; SP, subplate.

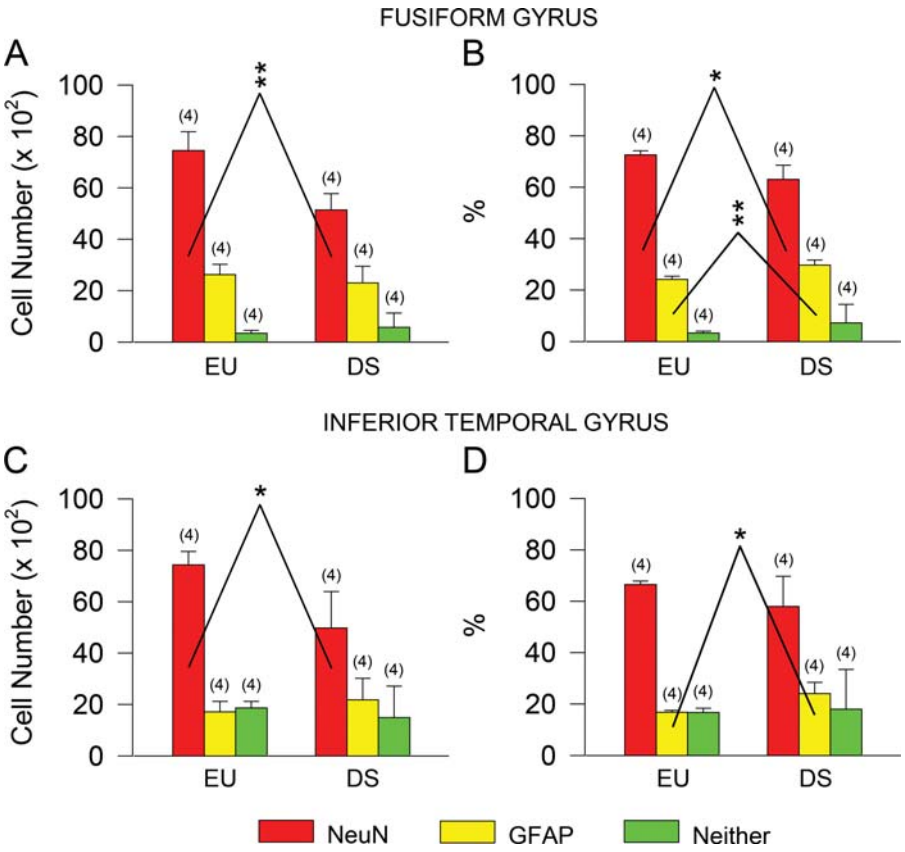

Figure 4. *Neurons and astrocytes in the fusiform gyrus and inferior temporal gyrus of DS and euploid fetuses.* **A–D**. Total number (A,C) and percentage (B,D) of NeuN-positive cells (red bars), GFAP-positive cells (yellow bars) and cells that did not express either NeuN or GFAP (green bars) in the cortical plate of the fusiform gyrus (A,B) and inferior temporal gyrus (C,D) of DS (n = 4; GW18, GW19, GW20, GW21) and euploid (n = 4; GW17, GW19, GW20, GW21) fetuses. Values are mean ± SD. The number in parentheses indicates the number of samples analyzed for each experimental group. * $P < 0.05$; ** $P < 0.01$ (two tailed *t*-test). Abbreviations: EU, euploid; DS, Down syndrome.

4A,C with Figure 5B,C). A comparison of euploid and DS fetuses showed that in DS fetuses the density of S100B-positive cells was larger than in euploid fetuses both in the FG and ITG, although the difference was significant for the ITG only (Figure 5B,C). An evaluation of the percentage of S100B-positive cells over total cell number showed that DS fetuses had a higher percentage of S100B-positive cells both in the FG (Figure 5B) and ITG (Figure 5C). We found scattered cells immunopositive for vimentin in the cortical plate of the FG and ITG. In absolute terms, their density was about one half than that of S100B-positive cells. An evaluation of the density and percentage of vimentin-positive cells showed no difference between euploid and DS fetuses both in the FG (Figure 5D) and ITG (Figure 5E). The cells immunopositive for S100B and vimentin found in the FG and ITG may account for the cells with an undetermined phenotype reported in Figure 4B,D. The possibility can also be taken into account that some of the cells with an undetermined phenotype include microglial cells.

Density and percentage of calretinin-positive cells in the FG and ITG of fetuses with DS

Calretinin (CR), which is a marker of inhibitory GABAergic interneurons, has been shown to be expressed at early stages of embryonic (18) and fetal (3) brain development and is one of the earliest neuroanatomical markers in human corticogenesis (18). While the principal neurons of the cortex originate in the ventricular zone, the inhibitory interneurons derive from the medial and caudal ganglionic eminences, with CR-positive neurons mainly deriving from the caudal ganglionic eminence (2, 18).

In sections subjected to immunohistochemistry for CR, CR-immunoreactivity was present throughout the whole ventral temporal lobe (Figure 1A), both in the cortical plate and marginal zone (Figures 1B,C and 3A,B). Scattered CR-positive cells were also present in the subplate region (data not shown), most likely representing migrating cells directed to the developing cortical plate. CR-positive cells in the cortical plate had a fusiform shape and could be of large size (Figure 1G) or relatively small size and orientation parallel (Figure 1G,H) or oblique (Figure 1I) with respect to the long axis of the cortical plate. In the marginal zone, CR-positive cells had either fusiform or rounded shape (Figure 6B).

In the cortical plate of the FG and ITG, CR-positive cells were largely outnumbered by CR-negative cells (Figure 6A). Quantification of the number of CR-positive and CR-negative cells showed no difference between euploid and DS fetuses in the density of CR-positive cells (Figure 6C,I). DS fetuses, however, had fewer CR-negative cells in comparison with euploid fetuses (Figure 6D,J).

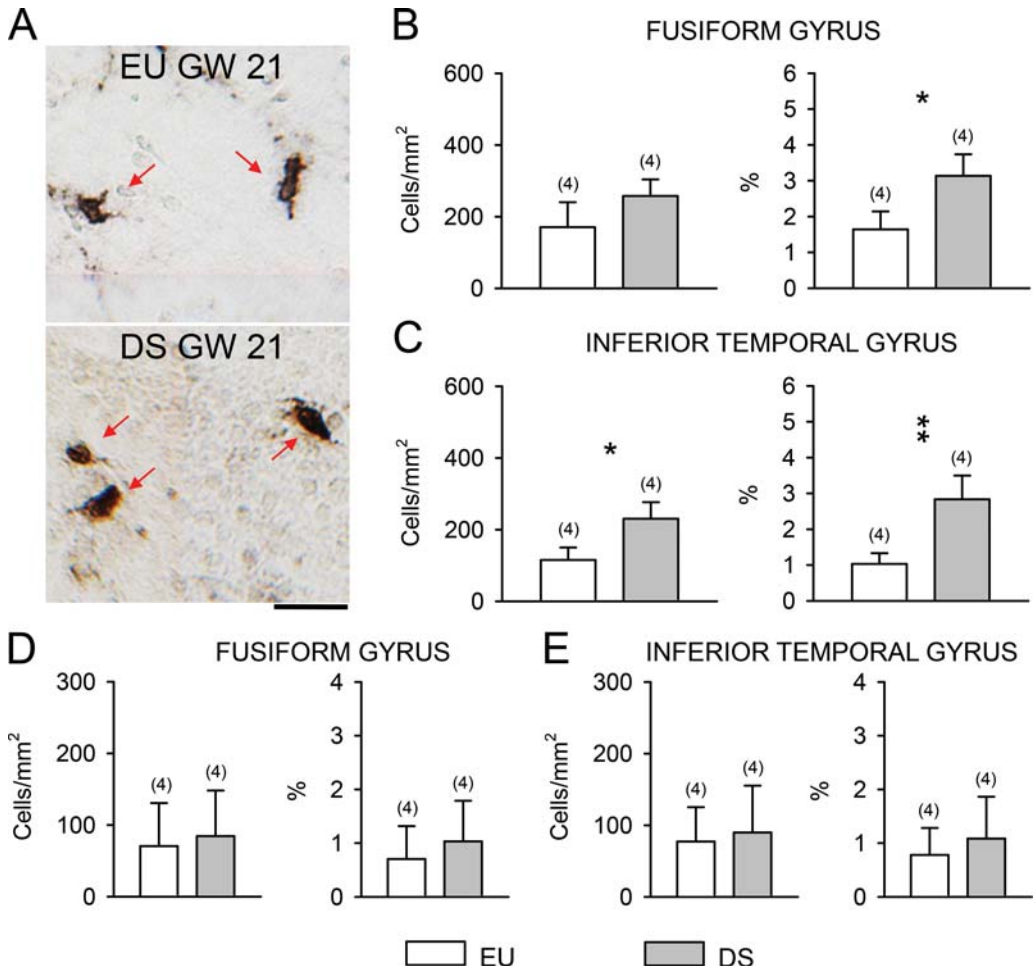

Figure 5. *Cells immunoreactive for S100B and vimentin in the fusiform gyrus and inferior temporal gyrus of DS and euploid fetuses.* **A**. Examples of S100B-positive cells (indicated by red arrows) in the fusiform gyrus of a euploid and a DS fetus of the same gestational age (GW21). Calibration = 20 μm. **B,C**. Density (left panel) and percentage (right panel) of S100B-positive cells in the cortical plate of the fusiform gyrus (B) and inferior temporal gyrus (C) and of vimentin-positive cells in the cortical plate of the fusiform gyrus (**D**) and inferior temporal gyrus (E) of DS (n = 4; GW18, GW19, GW20, GW21) and euploid (n = 4; GW17, GW19, GW20, GW21) fetuses. Values are mean ± SD. The number in parentheses indicates the number of samples analyzed for each experimental group. * $P < 0.05$; ** $P < 0.01$ (two tailed *t*-test). Abbreviations: EU, euploid; DS, Down syndrome; GW, gestational week.

Consistently with these data, an evaluation of the percentage of CR-positive vs. CR-negative cells, showed that in DS fetuses the percentage was significantly larger than in euploid fetuses both in the FG (Figure 6E; +77%) and ITG (Figure 6K; +61%).

Cajal–Retzius cells are a class of neurons located in the marginal zone of the neocortex and hippocampus that in addition to expressing reelin may also express CR (13, 38). Unlike in the cortical plate, in the marginal zone, CR-positive and CR-negative cells were almost equally represented (Figure 6B). A quantification of the number of CR-positive cells in the marginal zone of the FG and ITG showed that their density was four to five times larger than in the cortical plate (see Figure 6C,F,I,L) and of the same order of magnitude as that of CR-negative cells (see Figure 6F,G,L,M). A comparison of the density of CR-positive cells in DS and euploid fetuses showed that, unlike in the cortical plate, euploid fetuses had more CR-positive cells than DS fetuses (Figure 6F,L), although this difference did not reach significance. No difference was found in the number of CR-negative cells (Figure 6G,M). An evaluation of the percentage of CR-positive vs. CR-negative cells in the marginal zone, showed that in euploid fetuses the percentage of CR-positive cells was significantly larger than in DS fetuses both in the FG (Figure 6H; +50%) and ITG (Figure 6N; +37%).

Number and percentage of calretinin-positive cells in the hippocampal region of fetuses with DS

Since there is no evidence regarding the number of CR-positive cells in the hippocampal region of the DS brain, we examined the number of CR-positive cells in two critical hippocampal structures, the entorhinal cortex (ENT) and the hippocampal formation (DG and CA1). Evaluation of the number of CR-positive cells of euploid and DS fetuses showed that DS fetuses had a similar number of CR-positive cells as typical fetuses in the cortical plate of the

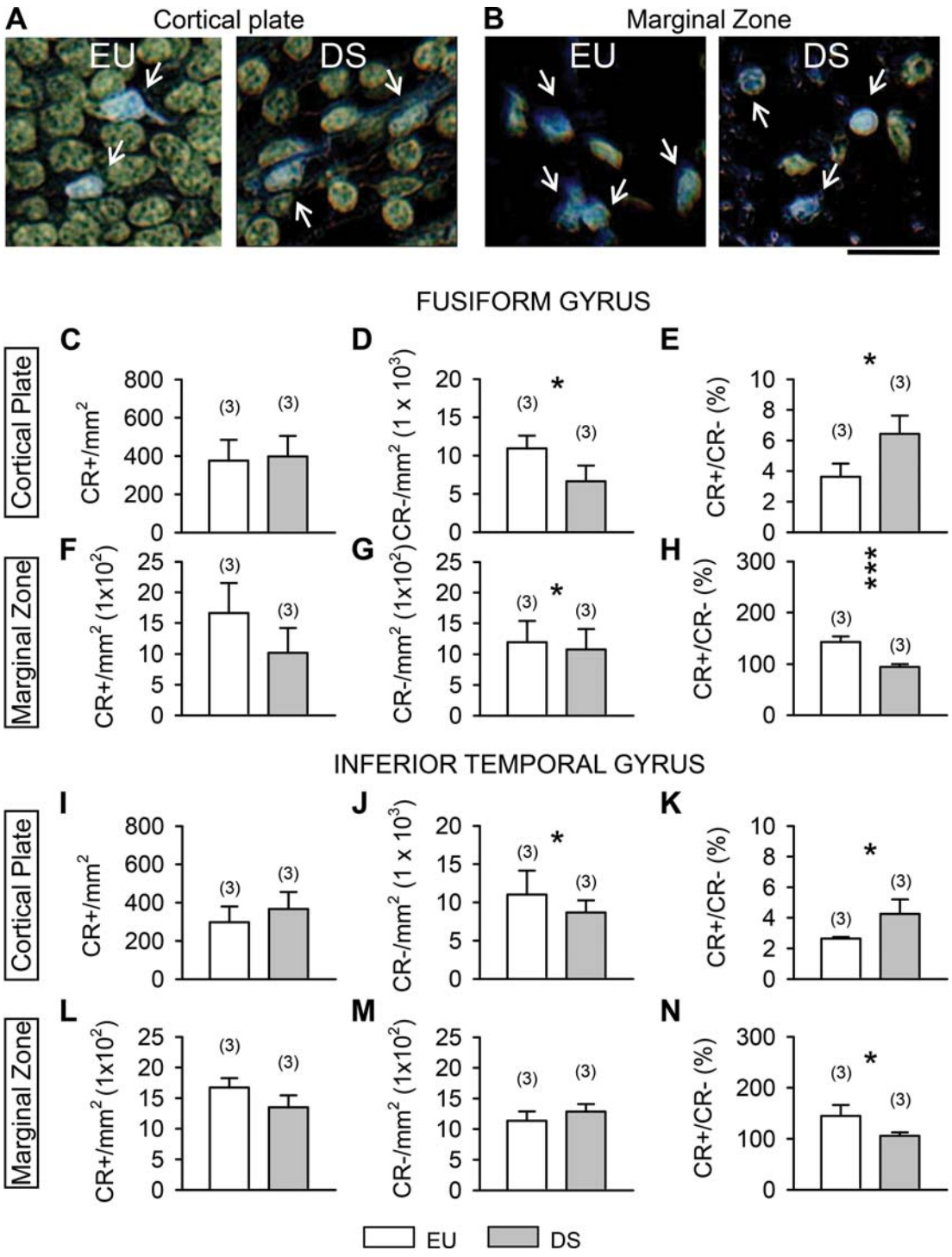

Figure 6. *Calretinin-positive cells in the fusiform gyrus and inferior temporal gyrus of DS and euploid fetuses.* **A,B**. Examples of calretinin-positive cells in the cortical plate (A) and marginal zone (B) of the inferior temporal gyrus of a euploid (C118; GW17) and a DS fetus (C203; GW 18). Sections were immunostained for calretinin and counterstained with hematoxylin. Colors have been inverted in order to better show calretinin-positive cells (blue cells indicated by white arrows). Calibration = 20 μm. **C–E, I–K**. Density of calretinin-positive cells (C,I), calretinin-negative cells (D,J) and ratio of calretinin-positive over calretinin-negative cells (E,K) in the cortical plate of the fusiform gyrus (C–E) and inferior temporal gyrus (I–K). **F–H, L–N**. Density of calretinin-positive cells (F,L), calretinin-negative cells (G,M) and ratio of calretinin-positive over calretinin-negative cells (H,N) in the marginal zone of the fusiform gyrus (F-H) and inferior temporal gyrus (L–N). DS fetuses: n = 3 (GW18, GW20, GW21). Euploid fetuses: n = 3 (GW17; GW20, GW20). Values are mean ± SD. The number in parentheses indicates the number of samples analyzed for each experimental group. * $P < 0.05$; *** $P < 0.001$ (two tailed *t*-test). Abbreviations: CR, calretinin; EU, euploid; DS, Down syndrome.

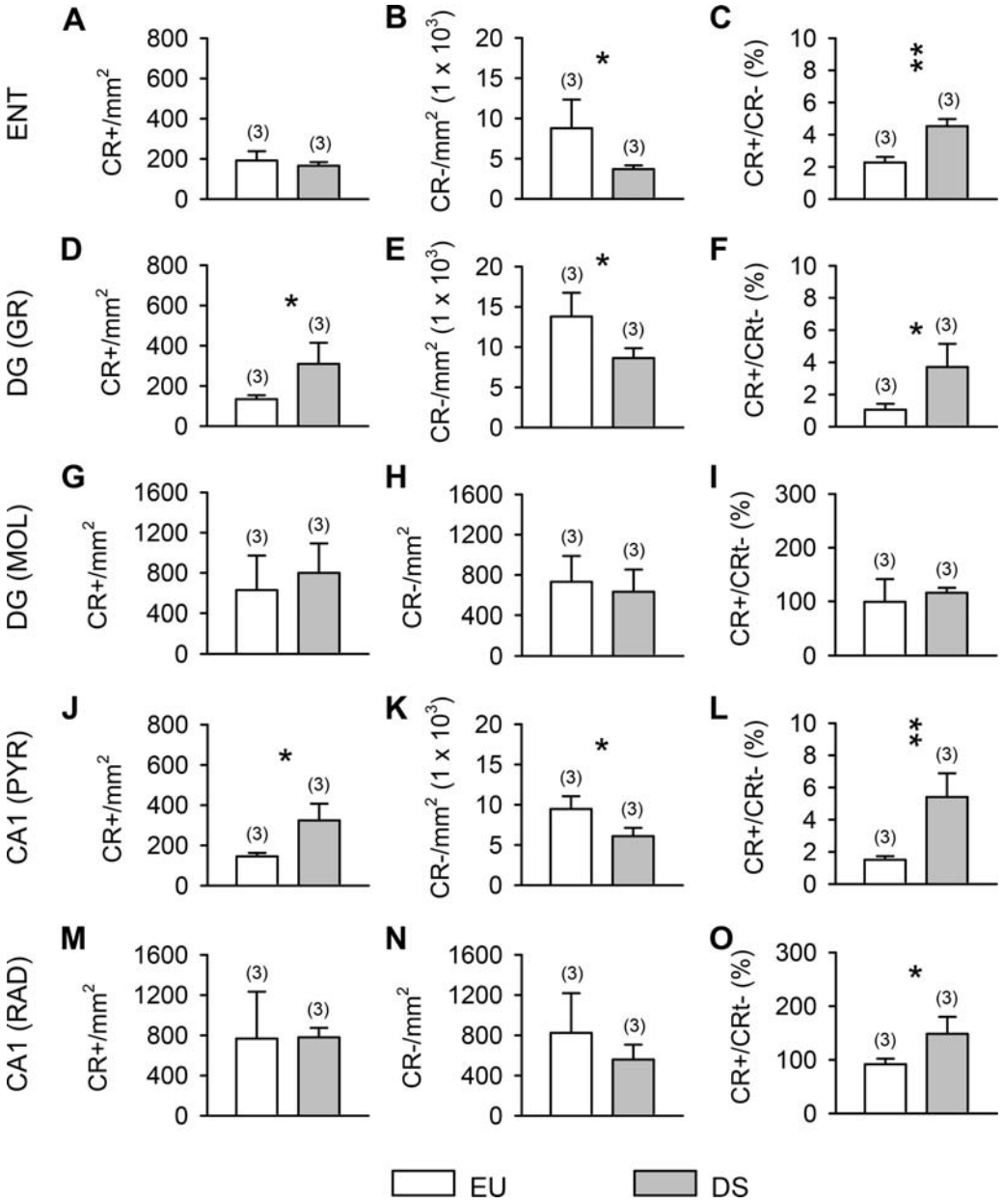

Figure 7. *Calretinin-positive cells in the entorhinal cortex and hippocampal formation of DS and euploid fetuses*. Density of calretinin-positive cells (**A,D,G,J,M**), calretinin-negative cells (**B,E,H,K,N**) and ratio of calretinin-positive over calretinin-negative cells (**C,F,I,L,O**) in the cortical plate of the entorhinal cortex (A–C), granule cell layer of the dentate gyrus (D–F), molecular layer (G–I) of the dentate gyrus, stratum pyramidale (J–L) and stratum radiatum (M–O) of field CA1. DS fetuses: n = 3 (GW18, GW20, GW21). Euploid fetuses: n = 3 (GW17; GW20, GW20). Values are mean ± SD. The number in parentheses indicates the number of samples analyzed for each experimental group. *$P < 0.05$; ** $P < 0.01$ (two tailed *t*-test). Abbreviations: CR, calretinin; DG, dentate gyrus; DS, Down syndrome; ENT, entorhinal cortex; EU, euploid; GR, granule cell layer; MOL, molecular layer, PYR, stratum pyramidale; RAD, stratum radiatum.

ENT (Figure 7A), in the molecular layer of the DG (Figure 7G) and in stratum radiatum of field CA1 (Figure 7M) but more CR-positive cells than control fetuses in the granule cell layer of the DG (Figure 7D) and in stratum pyramidale of field CA1 (Figure 7J). DS fetuses, however, had fewer CR-negative cells in the ENT (Figure 7B), granular layer of the DG (Figure 7E) and stratum pyramidale of field CA1 (Figure 7K) which is consistent with similar evidence obtained in the FG and ITG. No difference in the number of CR-negative cells was found in the molecular layer of the DG (Figure 7H) and stratum radiatum of field CA1 (Figure 7N) of euploid and DS fetuses. An evaluation of the percentage of CR-positive vs. CR-negative cells, showed that in DS fetuses the percentage was significantly larger than in euploid fetuses in the ENT (Figure 7C; +99%), granule cell layer of the DG (Figure 7F;

+350%), stratum pyramidale (Figure 7L; +260%) and stratum radiatum (Figure 7O; +62%) of field CA1. These findings are in line with results described above regarding the cortical plate of the FG and ITG. In contrast, no difference was found in the molecular layer of the DG (Figure 7I).

DISCUSSION

Abnormal architecture and reduced neuron number in the FG and ITG of DS fetuses

Results showed an overall reduction in cell density in the cortical plate of the FG and ITG of fetuses with DS accompanied by a thickness reduction, indicating an overall reduction in total cell number. The germinal matrix of the inferior horn of the lateral ventricle contains the precursor of neurons (NPCs) that will populate the regions of the ventral temporal lobe. A significantly reduced number of proliferating NPCs was previously found in the germinal matrix of the inferior horn of DS fetuses (11), which can account for the reduced cellularity observed here in the cortical plate of the FG and ITG.

Regarding the type of cells populating the fetal FG and ITG, results showed that most (~70% in euploid fetuses) of the cells populating the cortical plate were neurons (NeuN-positive cells). Most of the NeuN-negative cells expressed the astrocytic markers GFAP (~20% in euploid fetuses) and fewer cells expressed the astrocytic markers S100B (~1%–1.5% in euploid fetuses) and vimentin (<1% in euploid fetuses). The current finding of S100B-positive cells in the fetal temporal cortex is in agreement with a study showing the presence of S100B-positive cells in various regions of the fetal brain as early as GW15 (29). From the data reported in that study, it appears that the density of S100B-positive cells in the hippocampus, entorhinal cortex and occipital cortex of fetuses aged 21 weeks (29) is of the same magnitude as that found here in the temporal cortex. This corroborates our finding that only a small population of cells express S100B at early stages of cortical development. During fetal development, involution of ventricular processes of the radial glia cells and transformation into astrocytes takes place (12). This transformation may account for the vimentin-positive cells found here in the cortical plate of euploid and DS fetuses. The low number of vimentin-positive cells in comparison with GFAP-positive cells found here in fetuses aged 17–21 weeks is consistent with evidence that while brains of fetuses aged 14–16 weeks have a strong immunoreactivity for vimentin and weaker immunoreactivity for GFAP, the opposite takes place in fetuses aged 18–35 weeks (12).

A comparison of DS and euploid fetuses showed that DS fetuses had fewer neurons in comparison with euploid fetuses, a similar number of GFAP-positive cells and a larger number of S100B-positive cells in the FG and ITG. A reduced number of neurons with a relative increase in the number of astrocytes (GFAP-positive cells) has been detected across the whole hippocampal region of DS fetuses (20) as well as in the Ts65Dn model (7). The ensemble of these data suggests an alteration in the differentiation program that specifically compromises the generation of neurons. Alterations in the differentiation program are also suggested by studies showing that children with DS have even a higher number of astrocytes (detected with S100B-immunoreactivity) than typically developing children in the temporal lobe, in the frontal and occipital lobes and in the hippocampus (4, 19). While GFAP selectively labels astrocytes, S100B can be found in all glial cells (astrocytes, oligodendrocytes and microglia) (1, 26, 29). This suggests that the increased number of S100B-positive cells in DS fetuses may involve various aspects of glial function. The S100B protein is coded by one of the triplicated genes located on chromosome 21 and its expression has been shown to be upregulated in DS (19). While S100B can exert a variety of positive effects in the brain (14), its over expression may favor an increase in cytokine levels (19) and have, thus, detrimental effects on the brain. The increased number of S100B-positive cells found here in fetuses with DS suggests that excessive levels of S100B may have adverse effects on brain development.

Evidence in the Ts65Dn model of DS shows that cleavage products of the APP protein cause a reduction in the process of neurogenesis and favor the process of astrogliogenesis (30, 31). Increased APP levels have been detected in brains of fetuses with DS at the RNA (28) and protein (27) levels. Although various triplicated genes may affect the proliferation and fate of NPCs in the DS brain, this evidence suggests that early overexpression of APP may be a determinant of the altered proliferation and differentiation found in the ventral temporal region of fetuses with DS.

Increased number of calretinin-positive cells in the ventral temporal lobe of DS fetuses

The larger population (70%–80%) of neurons forming the cerebral cortex are excitatory neurons that use glutamate as a neurotransmitter and the smaller population are inhibitory interneurons that use GABA as neurotransmitter. Cortical GABAergic interneurons can be subdivided into three populations based on the expression of three different calcium-binding proteins, namely parvalbumin, calbindin and calretinin. In primates, CR-positive neurons are the most abundant interneuronal population (21). CR is expressed early in neocortical development, unlike other calcium-binding proteins which are predominantly expressed in the last trimester or postnatally [see (3)]. There is evidence that the distribution of CR-positive neurons is not homogeneous among different cortical areas (2, 3). Accordingly, observation of Figures 6 and 7 shows that the density of CR-positive neurons was different in different regions of the ventral temporal lobe both in euploid and DS fetuses. The relevance of these differences remains to be established.

In the cortical plate of the FG, ITG and ENT, in the granule cell layer of the DG and in stratum pyramidale of field CA1 the percentage of CR-positive neurons over the other cells present in these regions, most of which are neurons [see Figure 4A and (20)], was larger in DS than in euploid fetuses. This increase was due to a reduction in the number of CR-negative cells and not to an increase in the number of CR-positive cells, with the exception of the granular layer of the DG and stratum pyramidale of field CA1, where in absolute terms DS fetuses had more CR-positive cells than control fetuses. The finding that DS fetuses had a similar (or even larger) number of CR-positive cells as euploid fetuses suggests that the precursors of these cells do not share the same proliferation defects as the progenitors of the other neuron classes. CR-positive neurons arise from the ganglionic eminences (2, 18). In this connection, it seems of interest to observe that in the Ts65Dn model of DS inhibitory neurons derived from the medial ganglionic eminence, the

main source of forebrain inhibitory neurons, exhibit a higher proliferation rate in comparison with euploid mice (9).

Most (75%) of CR-positive cells in the human cortex are GABAergic (2). It is well-established that at early stages of brain development GABAergic transmission exerts depolarizing instead of hyperpolarizing effects (5). Although the synaptic connections and the role of CR-positive neurons in the fetal cortex remain to be established, the relative increase in the number of CR-positive cells in DS fetuses suggests possible alterations in the organization of cortical networks.

Abnormal distribution of CR-positive cells in the marginal zone of DS fetuses

Cajal–Retzius cells are a transient class of neurons that derive from multiple origins including ganglionic eminence and then migrate tangentially to the marginal zone (23). During cortical development, Cajal–Retzius cells synthesize and secrete the glycoprotein reelin that acts as a stop signal to regulate neuronal migration and is crucial for proper cortical development (16). Consistent with evidence that antibodies to CR label Cajal–Retzius cells during the period of corticogenesis (37), we found that the marginal zone of both euploid and DS fetuses contained a large population of cells that were immunopositive for CR. While in euploid fetuses CR-positive cells outnumbered the population that did not express CR, in DS fetuses CR-positive and CR-negative cells were roughly similar in number (see Figure 6). Although the significance of this difference remains to be established, it is tempting to speculate that abnormalities in the relative size of the population of CR-expressing cells in the marginal zone of DS fetuses may contribute to the abnormal cortical lamination observed in various regions of the fetal DS brain (4, 17).

CONCLUSIONS

Results indicate that in DS fetuses the FG and ITG are notably underdeveloped and disorganized in comparison with euploid fetuses. The cellularity reduction associated with an abnormal neuron to astrocyte ratio and an increase in the number of calretinin-positive neurons may underlie the functional alterations in visual recognition memory in children with DS. To our knowledge, this is the first demonstration that two regions critical for visual recognition memory are impaired in terms of cellularity and cell types. Previous evidence showed impaired development of the hippocampal region in fetuses with DS (20), a region that is crucial for explicit memory. The picture that emerges from our current and previous study (20) suggests that the fetal DS brain is characterized by a generalized impairment in the memory systems of the ventral temporal lobe, which can account for the deficits in different memory domains observed in children (and adults) with DS.

ACKNOWLEDGMENT

Support by Fondazione del Monte, Bologna, Italy is gratefully acknowledged. The assistance of Melissa Stott in the revision of the language and the technical assistance of Mr. Francesco Campisi and Mr. Massimo Verdosci are gratefully acknowledged.

REFERENCES

1. Adami C, Sorci G, Blasi E, Agneletti AL, Bistoni F, Donato R (2001) S100B expression in and effects on microglia. *Glia* **33**:131–142.
2. Barinka F, Druga R (2010) Calretinin expression in the mammalian neocortex: a review. *Physiol Res* **59**:665–677.
3. Bayatti N, Moss JA, Sun L, Ambrose P, Ward JF, Lindsay S, Clowry GJ (2008) A molecular neuroanatomical study of the developing human neocortex from 8 to 17 postconceptional weeks revealing the early differentiation of the subplate and subventricular zone. *Cereb Cortex* **18**:1536–1548.
4. Becker L, Mito T, Takashima S, Onodera K (1991) Growth and development of the brain in Down syndrome. *Prog Clin Biol Res* **373**: 133–152.
5. Ben-Ari Y, Khalilov I, Represa A, Gozlan H (2004) Interneurons set the tune of developing networks. *Trends Neurosci* **27**:422–427.
6. Bi Y, Wang X, Caramazza A (2016) Object domain and modality in the ventral visual pathway. *Trends Cogn Sci* **20**:282–290.
7. Bianchi P, Ciani E, Guidi S, Trazzi S, Felice D, Grossi G *et al* (2010) Early pharmacotherapy restores neurogenesis and cognitive performance in the Ts65Dn mouse model for Down syndrome. *J Neurosci* **30**:8769–8779.
8. Carlesimo GA, Marotta L, Vicari S (1997) Long-term memory in mental retardation: evidence for a specific impairment in subjects with Down's syndrome. *Neuropsychologia* **35**:71–79.
9. Chakrabarti L, Best TK, Cramer NP, Carney RS, Isaac JT, Galdzicki Z, Haydar TF (2010) Olig1 and Olig2 triplication causes developmental brain defects in Down syndrome. *Nat Neurosci* **13**: 927–934.
10. Chapman RS, Hesketh LJ (2000) Behavioral phenotype of individuals with Down syndrome. *Ment Retard Dev Disabil Res Rev* **6**:84–95.
11. Contestabile A, Fila T, Ceccarelli C, Bonasoni P, Bonapace L, Santini D *et al* (2007) Cell cycle alteration and decreased cell proliferation in the hippocampal dentate gyrus and in the neocortical germinal matrix of fetuses with Down syndrome and in Ts65Dn mice. *Hippocampus* **17**:665–678.
12. deAzevedo LC, Fallet C, Moura-Neto V, Daumas-Duport C, Hedin-Pereira C, Lent R (2003) Cortical radial glial cells in human fetuses: depth-correlated transformation into astrocytes. *J Neurobiol* **55**:288–298.
13. del Rio JA, Martinez A, Fonseca M, Auladell C, Soriano E (1995) Glutamate-like immunoreactivity and fate of Cajal-Retzius cells in the murine cortex as identified with calretinin antibody. *Cereb Cortex* **5**: 13–21.
14. Donato R, Cannon BR, Sorci G, Riuzzi F, Hsu K, Weber DJ, Geczy CL (2013) Functions of S100 proteins. *Curr Mol Med* **13**:24–57.
15. Fernández-Alcaraz C, Extremera MR, García-Andres E, Fernando, Molina C (2010) Emotion recognition in Down's syndrome adults: neuropsychology approach. *Procedia - Soc Behav Sci* **5**:2072–2076.
16. Gil-Sanz C, Franco SJ, Martinez-Garay I, Espinosa A, Harkins-Perry S, Muller U (2013) Cajal-Retzius cells instruct neuronal migration by coincidence signaling between secreted and contact-dependent guidance cues. *Neuron* **79**:461–477.
17. Golden JA, Hyman BT (1994) Development of the superior temporal neocortex is anomalous in trisomy 21. *J Neuropathol Exp Neurol* **53**: 513–520.
18. Gonzalez-Gomez M, Meyer G (2014) Dynamic expression of calretinin in embryonic and early fetal human cortex. *Front Neuroanat* **8**:41.
19. Griffin WS, Stanley LC, Ling C, White L, MacLeod V, Perrot LJ *et al* (1989) Brain interleukin 1 and S-100 immunoreactivity are elevated in Down syndrome and Alzheimer disease. *Proc Natl Acad Sci U S A* **86**: 7611–7615.
20. Guidi S, Bonasoni P, Ceccarelli C, Santini D, Gualtieri F, Ciani E, Bartesaghi R (2008) Neurogenesis impairment and increased cell death

reduce total neuron number in the hippocampal region of fetuses with Down syndrome. *Brain Pathol* **18**:180–197.
21. Hladnik A, Dzaja D, Darmopil S, Jovanov-Milosevic N, Petanjek Z (2014) Spatio-temporal extension in site of origin for cortical calretinin neurons in primates. *Front Neuroanat* **8**:50.
22. Honig LS, Herrmann K, Shatz CJ (1996) Developmental changes revealed by immunohistochemical markers in human cerebral cortex. *Cereb Cortex* **6**:794–806.
23. Martinez-Cerdeno V, Noctor SC (2014) Cajal, Retzius, and Cajal-Retzius cells. *Front Neuroanat* **8**:48.
24. Mesulam MM (1998) From sensation to cognition. *Brain* **121**: 1013–1052.
25. Nadel L (2003) Down's syndrome: a genetic disorder in biobehavioral perspective. *Genes Brain Behav* **2**:156–166.
26. Steiner J, Bernstein HG, Bielau H, Berndt A, Brisch R, Mawrin C *et al* (2007) Evidence for a wide extra-astrocytic distribution of S100B in human brain. *BMC Neurosci* **8**:2.
27. Tanzi RE, Gusella JF, Watkins PC, Bruns GA, St George-Hyslop P, Van Keuren ML *et al* (1987) Amyloid beta protein gene: cDNA, mRNA distribution, and genetic linkage near the Alzheimer locus. *Science (New York, NY)* **235**:880–884.
28. Tanzi RE, McClatchey AI, Lamperti ED, Villa-Komaroff L, Gusella JF, Neve RL (1988) Protease inhibitor domain encoded by an amyloid protein precursor mRNA associated with Alzheimer's disease. *Nature* **2**:383–330.
29. Tiu SC, Chan WY, Heizmann CW, Schafer BW, Shu SY, Yew DT (2000) Differential expression of S100B and S100A6(1) in the human fetal and aged cerebral cortex. *Brain Res Dev Brain Res* **119**:159–168.
30. Trazzi S, Fuchs C, Valli E, Perini G, Bartesaghi R, Ciani E (2013) The amyloid precursor protein (APP) triplicated gene impairs neuronal precursor differentiation and neurite development through two different domains in the Ts65Dn mouse model for Down syndrome. *J Biol Chem* **288**:20817–20829.
31. Trazzi S, Mitrugno VM, Valli E, Fuchs C, Rizzi S, Guidi S *et al* (2011) APP-dependent up-regulation of Ptch1 underlies proliferation impairment of neural precursors in Down syndrome. *Hum Mol Genet* **20**:1560–1573.
32. Vicari S (2004) Memory development and intellectual disabilities. *Acta Paediatr Suppl* **93**:60–63.
33. Vicari S (2006) Motor development and neuropsychological patterns in persons with Down syndrome. *Behav Genet* **36**:355–364.
34. Vicari S, Bellucci S, Carlesimo GA (2000) Implicit and explicit memory: a functional dissociation in persons with Down syndrome. *Neuropsychologia* **38**:240–251.
35. Visu-Petra L, Benga O, Ţincaş I, Miclea M (2007) Visual-spatial processing in children and adolescents with Down's syndrome: a computerized assessment of memory skills. *J Intellect Disabil Res* **51**: 942–952.
36. Weiner KS, Zilles K (2016) The anatomical and functional specialization of the fusiform gyrus. *Neuropsychologia* **83**:48–62.
37. Weisenhorn DM, Prieto EW, Celio MR (1994) Localization of calretinin in cells of layer I (Cajal-Retzius cells) of the developing cortex of the rat. *Brain Res Dev Brain Res* **82**:293–297.
38. Weisheit G, Gliem M, Endl E, Pfeffer PL, Busslinger M, Schilling K (2006) Postnatal development of the murine cerebellar cortex: formation and early dispersal of basket, stellate and Golgi neurons. *Eur J Neurosci* **24**:466–478.